ELSEVIER

Polymer 43 (2002) 3123–3129

polymer

www.elsevier.com/locate/polymer

Polymer Communication

# Modification of poly(*N*-vinyl-carbazole) thin films by bromine doping

S. Touihri[a], J.C. Bernède[b,*], P. Molinie[c], D. Legoff[d]

[a]*LPMC, Faculté des Sciences de Tunis, Campus Universitaire, Tunisie, France*
[b]*GL, LPSE-FSTN, Universite de Nantes, GPSE, Equipe Couches Minces et Materiaux Nouveaux, FSTN BP 92208, 2 Rue de la Houssiniere, 44072 Nantes Cedex 3, France*
[c]*LCS-IMJR, BP 92208, Fr-44322 Nantes Cedex 3, France*
[d]*Chemical IUP, FSTN, 2 Rue de la Houssinière, BP 92208, Fr-44322 Nantes Cedex 3, France*

Received 23 July 2001; received in revised form 31 January 2002; accepted 5 February 2002

---

**Abstract**

Poly(*N*-vinyl-carbazole) (PVK) thin films doped with bromine has been studied by scanning electron microscopy, X-ray diffraction, infrared absorption, X-ray photoelectron spectroscopy (XPS), electron spin resonance (ESR), optical transmission (visible, near ultra violet) and conductivity measurements. The polymer has been doped at room temperature and at 373 K. It is shown by ESR, XPS and optical measurements that a charge transfer complex (CT-complex) is formed between PVK and Br. However, if some bromine acts as dopant of the polymer there is another bromine contribution, which corresponds to bromine covalently bonded to PVK and some only adsorbed. It is also shown by ESR that there is not only polymer doping by bromine but also some partial polymer degradation. Therefore, it can be said that the optimum doping condition of PVK thin films with bromine has been shown to be room temperature post-doping. © 2002 Elsevier Science Ltd. All rights reserved.

*Keywords*: Poly(*N*-vinyl-carbazole); Thin film; Evaporation

---

## 1. Introduction

Many authors have investigated the poly(*N*-vinyl-carbazole) (PVK) since the discovery, in 1957, of its photoconduction [1,2]. More recently many works have been done on the luminescence properties of PVK. Electroluminescent diodes based on PVK, which emits blue light, have been extensively studied [3–8]. The success of the investigations in this field of organic electroluminescent diodes (OLED) has induced a new interest to organic photovoltaic diodes [9,10]. In order to obtain reasonable efficiency, it has been shown that such photoactive device is based on the photo-induced electron transfer from donor type polymer to acceptor molecules. Encouraging efficiency is activated by mixing electron-donor type polymer with suitable electron acceptor. In such single layer photoactive mixture film, a 'bulk' heterojunction is formed between the electron donors and acceptors [9].

Moreover, the polymer itself should exhibits some specific properties such as optical absorption in the visible domain. One way to improve the properties of this polymer for photovoltaic application is to form a charge transfer complex (CT-complex) between PVK and a dopant. The PVK is an electron donor and the dopant should be an electron acceptor. As discussed earlier for photovoltaic effect, the absorption of the CT-complex should not be negligible in the visible part of the spectrum.

We have shown earlier that the formation of a complex salt with iodine strongly improves the conductivity of the PVK, while a broad absorption appears in the visible domain [11–13]. However, it is difficult to stabilize the properties of these complex salts by post-annealing treatment, because annealing of PVK under iodine atmosphere induces PVK degradation. In the case of chlorine, even when doped at room temperature, there is polymer degradation [14]. In the case of bromine doping, intermediate results are obtained. The stability of the CT-complex obtained after doping is higher than that of iodine doped polymer but the degradations induced by doping are far smaller than those induced by chlorine [15,16].

We have also shown that PVK thin films can be obtained by vacuum evaporation [17]. A systematical study of these films demonstrates that thermal evaporation has a shortening effect on the polymer chains, while the vinyl-carbazole

---

* Corresponding author. Address: LPSE-FSTN, BP 92208, Fr-44322 Nantes Cedex 3, France. Tel.: +33-2-51-12-55-30; fax: +33-2-51-12-55-28.

*E-mail address:* jean-christian.bernede@physique.univ-nantes.fr (J.C. Bernède).

PII: S0032-3861(02)00118-0

function is preserved [18,19]. It was also shown that halogen doped films with the best properties are obtained by doping the PVK after evaporation and not before [18,21]. Moreover, we have shown that, as in the case of spin coating films, evaporated PVK films in glass/$SnO_2$/PVK/Al sandwich structures allows to obtain OLED, which emit blue light as expected for such molecule [22,23].

Therefore in the present work, we report the study of evaporated PVK thin films doped, after evaporation, by bromine.

## 2. Experimental

### 2.1. Thin film deposition and doping

PVK and bromine were provided by Aldrich, with a purity of 99.99%. The PVK films were obtained by the evaporation of PVK powder, under a vacuum better than $10^{-5}$ Pa, from a molybdenum boat. This boat has a special configuration (two superposed multi-holed covers) to avoid the projection of the PVK powder at the beginning of the heating. The evaporation temperature was measured by a chromel alumel thermocouple at a temperature around 590 K.

The substrates were soda lime glass, for X-ray diffraction (XRD), scanning electron microscopy (SEM) and conductivity measurements, silica slides for visible, near ultra violet transmission measurements and electron spin resonance (ESR) measurements. NaCl single crystals for infrared (IR) absorption and stainless steel plates for X-ray photoelectron spectroscopy (XPS) studies.

Since it has been shown that the morphology of the layers depends strongly on the cleanliness of the substrates [17], they have been very carefully cleaned before deposition. The NaCl has been cleaved just before it was introduced into the bell jar under vacuum, while glass and silica have been cleaned by using alcohol in ultrasonic sound bath, then HCl solution and finally distilled water heated at 373 K. The samples are dried in a nitrogen flow.

Before evaporation, the substrates were heated at $T = 400$ K for 1 h to disorber the water vapor. During the deposition, the substrate holder temperature was 300 K. The temperature was controlled by a copper-constantan thermocouple attached by silver paste to the surface of the sample. Prior to deposition, the molybdenum boat was slowly heated to degas the PVK powder. The evaporation rate (1 nm $s^{-1}$) and the film thickness (1–5 μm) were measured in situ using the vibrating quartz method. After deposition, in order to dope the thin films, they were introduced, with a small capillary tube full of bromine, into previously outgassed Pyrex tube. After sealing under vacuum, the tube was gently shaken to break the brittle bromine capillary tube. Then the ampoule was either kept at room temperature or heated at 373 K for 24 h. While before doping the films were transparent, they become lightly brown colored after doping.

Some measurements have been done on solution of $Br_2$ and PVK. In that case, we proceed as follows. First PVK powder was introduced, with a small capillary tube full of bromine, in a fused quartz tube previously outgassed. This tube sealed under vacuum was then shaken in order to break the bromine capillary tube. The quartz ampoule was heated at $270 \leq T \leq 370$ K for 24 h.

Then this powder was dissolved in tetrahydrofuran (THF) or in tetrachlorure ($CDCl_4$). It should be noted that the PVK solubility is quite small in these solvents.

Pure and bromine doped PVK solutions have been characterized by IR absorption and nuclear magnetic resonance (NMR).

### 2.2. Thin film characterization

Observation of the morphology of the layers was performed using a JEOL 6400F field effect SEM. The optical measurements were carried out at room temperature for visible and near ultra violet domains using a carry spectrophotometer. The optical density was measured at wavelengths 2–0.3 μm. These optical measurements were carried out in the Laboratory of Crystalline Physics, Institute of Materials of Nantes (LPC-IMN).

The IR absorption spectra were recorded using a FTIR spectrometer. Absorption band positions are given in waves numbers ($cm^{-1}$). In the case of solutions, a 89 μm KBr cell has been used.

The structure of the films was checked by an X-ray diffractometer using an X-ray system-type, diffract AT V3 Siemens instrument, which uses a graphics program EVA. The wavelength $\lambda$ was 1.5406 A.

ESR experiments were performed at ambient temperature on a Bruker ER 200D spectrometer operating at X band. The decomposition of the ESR spectrum and the interpretation were made using the method described elsewhere [24,25]. Using the pole method integration [26] with a Gaussian or a Lorentzian or a mixture of the two line shape, the theoretical ESR signal can be computed yielding parameters of each distribution that can produce the signal after comparison with experimental results.

XPS measurements were performed with a magnesium X-ray source (1253.6 eV) operating at 10 kV and 10 mA. The energy resolution was 0.75 eV at a pass energy of 50 eV.

The quantitative XPS study was based on the determination of the C1s, N1s, Br3d and O1s peak areas with 0.2, 0.36, 0.67 and 0.61, respectively, as sensibility factors (the sensitivity factors were given by the manufacturer (Leybold)). The decomposition of the XPS peaks into different components and the quantitative interpretation were made after subtraction of the background using the Shirley method [27]. The developed curve-fitting programs permit the variation of parameters such as the Gaussian/Lorentzian ratio, the full width at half maximum (FWHM), the position and the intensity of the contribution. These parameters were optimized by the curve-fitting program in order to obtain the best fit.

Some etching of the films have been done to check the bromine distribution. Using an ion gun, etching was accomplished at pressures of less than $5 \times 10^{-4}$ Pa with a 10 mA emission current and 5 kV beam energy. The $\mathrm{Ar}+$ ion beam was rastered over the entire sample surface.

1H NMR (100 MHz) spectra were recorded on a Varian XL 100 spectrometer. TMS was used as the internal standard and $CDCl_3$, $CD_3$–CO–$CD_3$ as solvent and lock.

Conductivity measurements were carried out on planar structures. The metallic electrodes used were evaporated gold electrodes. Resistance measurements were performed at room temperature in the dark with an electrometer (Keithley). The electrical conductivity of the films was calculated from these resistance measurements.

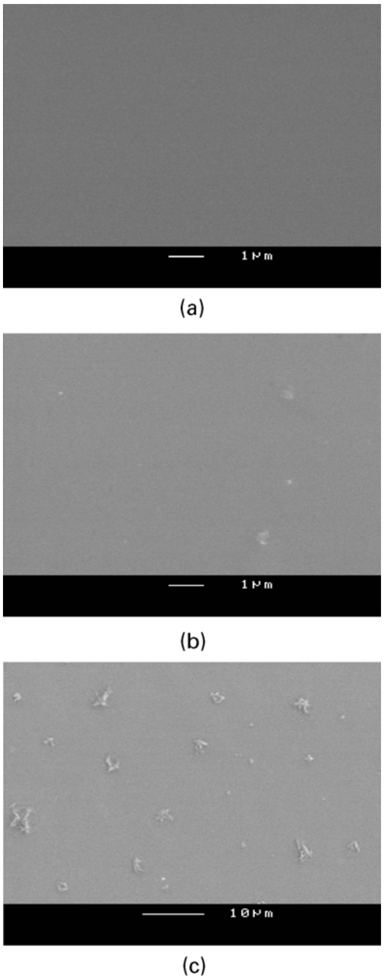

(a)

(b)

(c)

Fig. 1. Scanning electron micrographs of films deposited on soda lime glass substrates. (a) Pure PVK film. (b) Bromine doped PVK film at room temperature. (c) Bromine doped PVK film at 373 K.

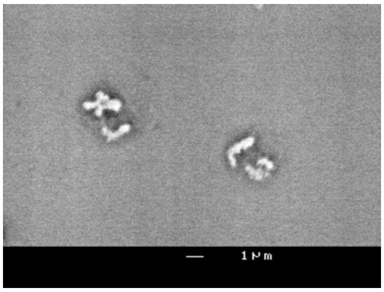

Fig. 2. Micrograph of a PVK film doped at 373 K, in the backscattered electron mode.

## 3. Experimental results

The properties of the evaporated films doped with bromine at room temperature and at 373 K will be described in this section and then they will be discussed in the light of the results obtained, with pure evaporated PVK films and with bromine doped PVK powder.

### 3.1. Morphological and structural study

The scanning electron micrographs in Figs. 1 and 2 show films of 1 μm thickness.

Whatever the substrate is, the pure PVK films are homogeneous and smooth as shown in Fig. 1(a). It can be seen that the layers are homogeneous and smooth (Fig. 1(a)). The corresponding X-ray diffractogram corresponds to

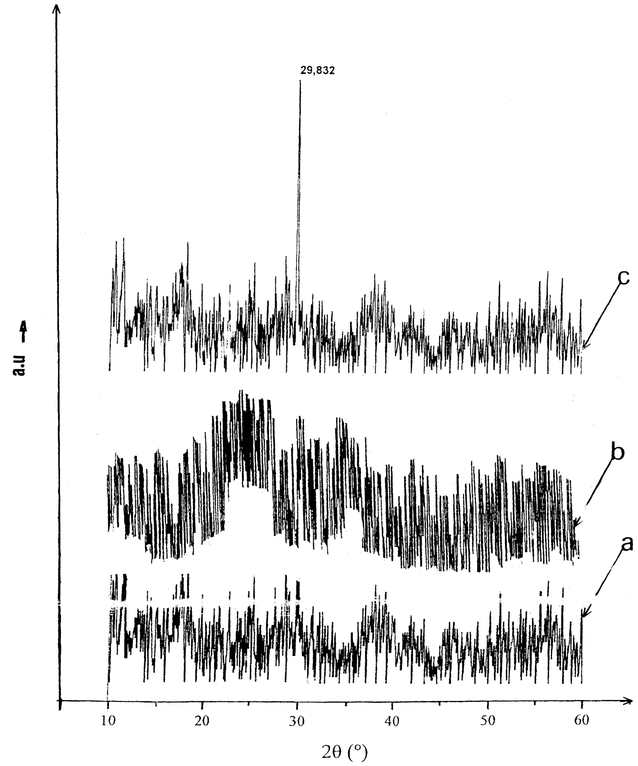

Fig. 3. X-ray diffractograms of different PVK samples. (a) Pure PVK film. (b) PVK film doped at room temperature. (c) PVK film doped at 373 K.

amorphous samples (Fig. 3(a)). After bromine doping at room temperature, the films are still homogeneous even if some features appears on the micrograph (Fig. 1(b)), the X-ray diffractogram (Fig. 3(b)) stay typical of an amorphous film. After bromine doping at 373 K, the morphology of the layers is disturbed by granular features distributed randomly all over the sample (Fig. 1(c)).

It can be seen in Fig. 2 that, in the backscattered electron mode, the small features randomly distributed all over the films appear brighter than the film matrix, i.e. they corresponds to heavier elements.

Moreover, it can be seen in Fig. 3(c) that a diffraction peak appears at $2\theta = 29.73$. This peak can be attributed to the tetragonal $NH_4Br$ (JCPDS 85-0959) oriented along the (200) direction.

The crystallites are preferentially oriented along the (200) direction, since only the (200) peak appears. Such preferential orientation is not unusual in thin films.

### 3.2. Infrared absorption

The resolution of the spectra is far better in the case of powders dissolved in THF, than in the case of thin films. It can be seen in Fig. 4 that the main difference is the apparition of small absorption peaks between 700 and 750 $cm^{-1}$. These absorption peaks corresponds to C–Br bonds (Pouchert CJ. The Aldrich Library of FTIR spectra. Aldrich Company Inc., 1986: I.). This is the main information obtained from IR absorption study of PVK solutions. The resolution of the IR spectra of thin films is very poor as usual in thin films. They are not shown here; however, the main absorption bands of PVK are visible in the spectra. Among the carbon–carbon bonds, the typical C–N bond (1230 $cm^{-1}$) of the vinyl-carbazol function appears clearly in both spectra.

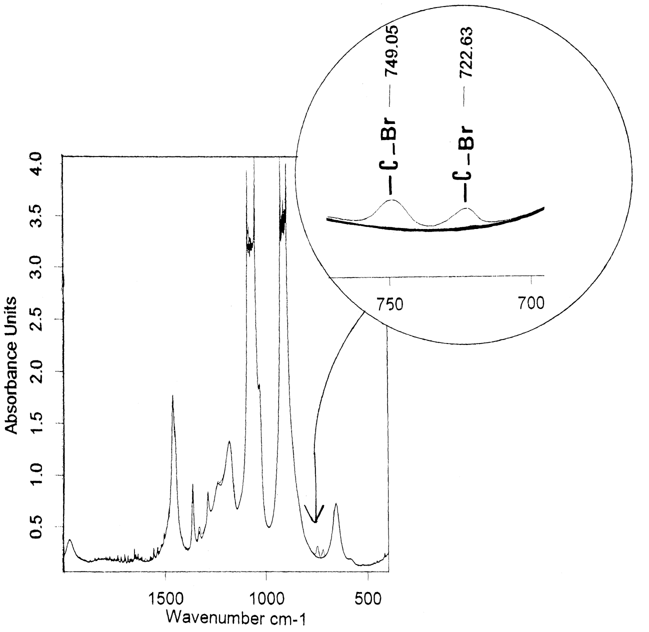

Fig. 4. IR absorption spectra of solutions of (▬) pure PVK; (—) PVK doped at 273 K.

Table 1
XPS quantitative analysis atomic concentration

| PVK thin films | C | N | Br | O |
|---|---|---|---|---|
| Pure PVK | 89 | 5 | | 6 |
| Pure PVK after one minute of etching | 95 | 2.5 | | 2.5 |
| Bromine doping at room temperature | 65 | 4 | 21 | 10 |
| Bromine doping at room temperature after one minute of etching | 79 | 2 | 13 | 6 |
| Bromine doping at 373 K | 55 | 4 | 32 | 9 |
| Bromine doping at 373 K after one minute of etching | 76 | 2 | 18 | 4 |

### 3.3. XPS analysis

In the incertitude range of the XPS technique, there is a good agreement between the theoretical and experimental N/C atomic ratio. This is true before and after doping. There is only 6–10 at% of contaminating oxygen at the surface of the films. It should be noted that oxygen contamination increases slightly after bromine doping. The relative atomic percentage of bromine presents at the surface of the film is quite large, it increases when the films are doped at 373 K. It can be checked in Table 1 that, as shown earlier [18], an etching destroys the C–N bonds and proceeds to a graphitization of the surface of the films. However, it can be seen that after etching of only 1 min, the relative atomic percentage of bromine decreases strongly which means that during doping some bromine is only surface absorbed.

The decomposition of the different XPS peaks are reported in Fig. 5 in the case of bromine doping of PVK thin films at room temperature. All the decompositions are reported in Table 2. Samples being quite resistive, there is some increase of the measured binding energy, which is called the charge effect $\Delta E$ (Table 2).

The C1s spectrum (Fig. 5(a)) skewed towards the highest energy side has been decomposed in three contributions. The first and main peak corresponds to carbon–carbon bond. In order to compare the binding energy of the different components of one sample from another, the values reported in the XPS decomposition table have been estimated by using the energy of this carbon–carbon bond as a reference, as is often the case in Ref. [17], with 285 eV as bonding energy. Therefore, for each sample, $\Delta E$ corresponds to the difference between the value experimentally measured and this reference value.

The second contribution corresponds to C–N bonds, since it is situated at 286 eV [28]. However, some C–OH bonds cannot be excluded. After doping the relative

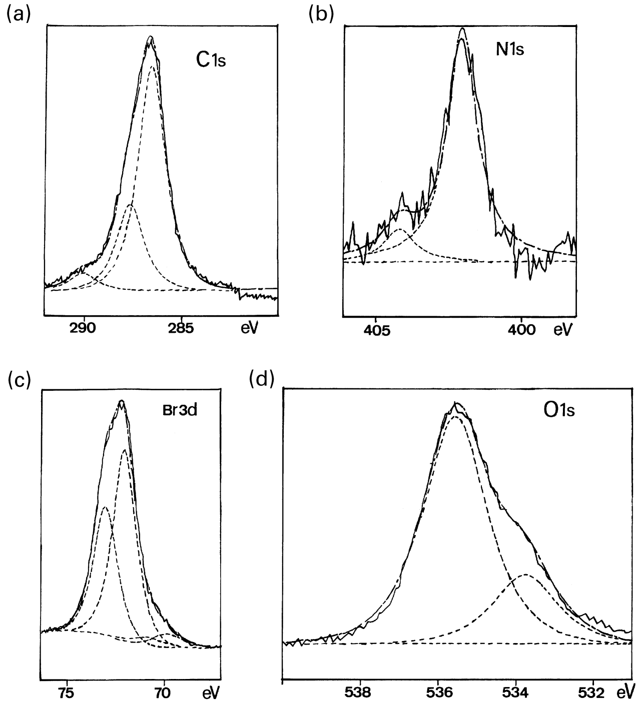

Fig. 5. XPS spectra of the (a) C1s, (b) N1s, (C) Br3d and (d) O1s, peaks after doping at room temperature.

intensity of this contribution increases which should be related to some $C^{\delta+}$ radical formation (Fig. 5(a)). The third peak corresponds to oxygen contamination.

Before doping the N1s peak situated at 400.4 eV can be assigned to the C–N covalent bond of the PVK. After doping a second contribution appears, it corresponds to positively charged nitrogen $N^{\delta+}$ (Fig. 5(b)).

Complementary information concerning the oxidation process can be obtained from the Br3d decomposition (Fig. 5(c)) (Table 2). Some broadening effect of the Br3d peak on the low energy side is visible. Therefore, one may expect this Br3d peak to originate from two different doublets superposed in such a way that the peak located at the smallest binding energy corresponds to the ionic state $Br^-$, while the other one is due to covalently bonded bromine. It can be seen that after etching (Fig. 6), the relative contribution of the ionic bromine increases (5–8 at% before etching, 25–30 at% after etching), which means that at the surface the main part of the bromine is covalently bonded to PVK and/or absorbed. This justifies the relatively high percentage of bromine, but it is shown that only a small part is active for PVK doping. There is a preferential etching of this absorbed bromine, which is only weakly bonded to the polymer and the ionic contribution increases relatively, while the whole bromine relative atomic concentration decreases. The covalently bonded Br which stays in the films after etching should corresponds to Br–PVK covalent peaks put in evidence by IR absorption study of Br–PVK solutions.

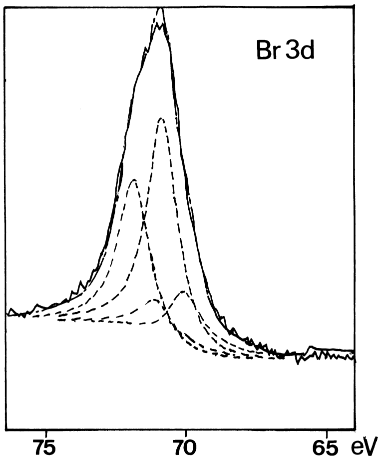

Fig. 6. XPS spectra of the Br3d peak of PVK doped at room temperature after an etching of 1 min. (‿⋀‿‿⋀‿) Experimental data; (—) theoretical curve; (- - -) different components.

The O1s peaks can also be decomposed into two components: the first one corresponds to C=O, while the second at higher energy can be attributed to C–O–H groups.

### 3.4. ESR and NMR studies

No ESR signal is observed for pure PVK powder and thin film before doping. After doping, a well-resolved ESR signal is systematically observed.

Since the ESR signal of bromine doped PVK powder has been broadly studied in a preceding paper [16], and since preceding experimental results show that a doping at 373 K destroy, at least partially, the polymer. The example of room

Table 2
XPS analysis of PVK samples (first row: binding energy (eV), second row: relative at%)

| PVK thin film sample | C1s | | | N1s | | O1s | | Br | |
|---|---|---|---|---|---|---|---|---|---|
| | C–C | C–N | C=Ox | $N^-$ | $N^+$ | | | $Br^-$ | Br |
| Pure PVK | 285 | 286 | 288 | 400.4 | | | | | |
| $\Delta E = 2$ eV | 78 | 18 | 4 | | | | | | |
| PVK doped with Br at room temperature | 285 | 286 | 288.5 | 400.4 | 402.6 | 531 | 533.5 | 68.5 | 70.5 |
| $\Delta E = 1.6$ eV | 70 | 25 | 5 | 83 | 17 | 25 | 75 | 8 | 92 |
| PVK doped with Br at 373 K | 285 | 286 | 289 | 400.4 | 402.4 | 530 | 533 | 68.5 | 70.2 |
| $\Delta E = 1.2$ eV | 52 | 43 | 5 | 87 | 13 | 13 | 87 | 6 | 94 |

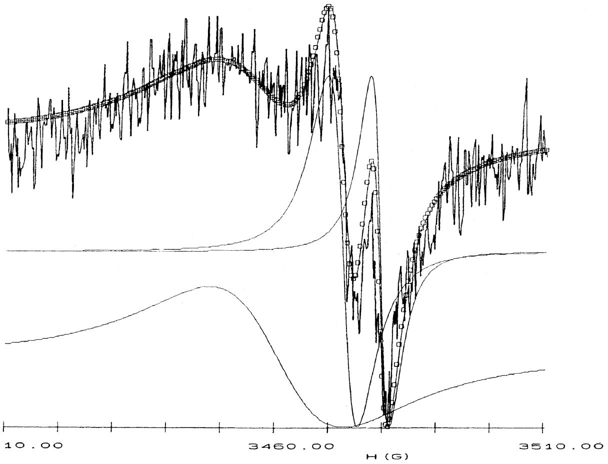

Fig. 7. ESR spectra: PVK thin film doped with bromine at room temperature. (⁀⁀) Experimental data; (—) theoretical curve; (- - -) different components.

temperature doped thin film only is reported (Fig. 7) and discussed in the light of the paper [16].

After doping at room temperature, the two main contributions and a small one are necessary to analyze the ESR spectrum. All distributions are isotropic.

The two main contributions with $g = 2.003$ and 2.001 are similar to the contributions called D1 and D3 in the PVK doped powder [16]. It has been shown in our preceding paper [16] that the D1 distribution ($g = 2.003$, FWAM = 6 G), can be attributed to carbon radicals on the backbone of the polymer as shown by the $g$ value [29]. This carbon radical on the backbone has been attributed to the polymer degradation during bromine doping [16]. The other contribution called D3 ($g = 2.001$, FWHM = 25 G) cannot correspond to a free radical. Therefore, this contribution has been attributed to the bromine doping, which corresponds to the expected CT-complex formation between PVK and Br [16]. The third contribution can be attributed to bromine interaction with backbone polymer defaults introduced during the evaporation process, which reduces the chain length.

If PVK is slightly soluble after doping, the only phase, which is soluble in chloroform and acetone as shown by NMR, is the $NH_4Br$.

However, it can be seen in Fig. 8 that these compounds are only present as traces since the signal intensity of these phases is of the same order of magnitude than that of impunities (acetone:$\delta = 2$ ppm) present in the glass tube containing the sample. Since it has become insoluble after bromine doping, the main part of the polymer cannot be analyzed by NMR which can only shows that $NH_4Br$ is present.

### 3.5. Optical transmission and conductivity measurements

The optical transmission spectra are reported in Fig. 9. It can be clearly seen that there is a broad red shift effect of the absorption threshold after bromine doping.

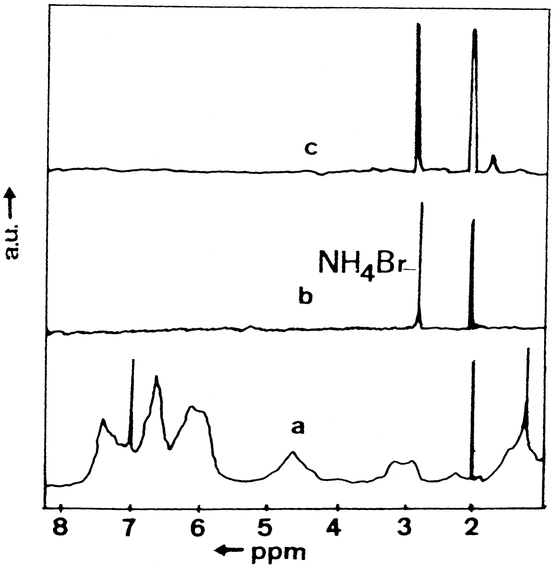

Fig. 8. NMR spectra of (a) pure PVK; (b) PVK powder doped at 273 K; (c) PVK powder doped at 373 K.

There is also a large increase of the conductivity after bromine doping. After 24 h at room temperature, the conductivity is $\sigma = 8.75 \times 10^{-6}$ $(\Omega\ \mathrm{cm})^{-1}$, moreover, the conductivity increases with the doping time. A saturation effect is obtained after three days and the conductivity stabilizes at $1.75 \times 10^{5}$ $(\Omega\ \mathrm{cm})^{-1}$.

In the case of doping at 373 K, the conductivity increase up to $10^{-7}$ $(\Omega\ \mathrm{cm})^{-1}$ after 24 h but then it decreases and it is $2.5 \times 10^{-8}$ $(\Omega\ \mathrm{cm})^{-1}$ after three days.

## 4. Discussion—conclusion

Thin films have been doped with bromine after deposition since it has been shown that the halogen doped PVK films are more homogeneous when they are post-doped [18–21].

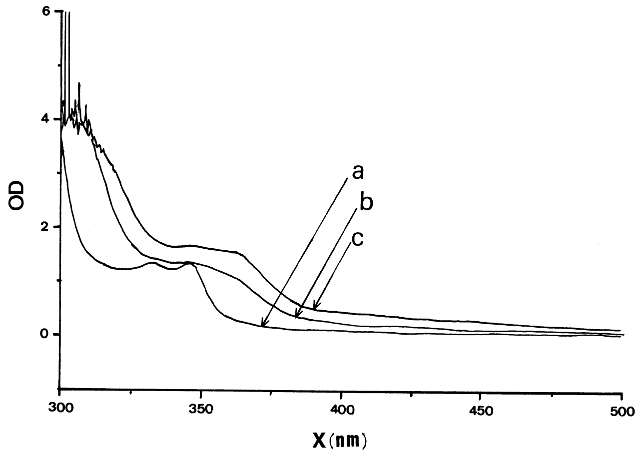

Fig. 9. Visible and near UV transmission spectra of (a) pure PVK thin films; (b) PVK thin film bromine doped at room temperature; (c) PVK thin film bromine doped at 373 K.

The films have been doped for 24 h at room temperature and at 373 K.

During doping at 373 K, it appears that bromine induces some polymer destruction as shown by the $NH_4Br$ presence in the films. In the case of room temperature doping, the PVK polymer is more preserved with clear CT-complex formation between Br and the polymer backbone as shown by the analysis of the XPS and ESR signals. However, it appears clearly that not only there is CT-complex formation between Br and PVK, but also as shown by XPS and IR absorption of Br–PVK solution, that there is Br–PVK covalent bonds formation, resulting in Ar–Br bonds.

The optical transmission spectra show that the expected effect, a red shift of the absorption threshold intervenes after bromine doping, which induces a broad absorption bond in the visible range.

The conductivity measurements corroborate the preceding study: a CT-complex is formed during doping at room temperature, which increases the sample conductivity up to a stable value of $1.75 \times 10^{-5}\ (\Omega\ \mathrm{cm})^{-1}$ reached after three days. In the case of doping at 373 K, the polymer partial destruction is corroborated by the increase of the conductivity during the first 24 h ($\sigma = 10^{-7}\ (\Omega\ \mathrm{cm})^{-1}$) and then a progressive decrease during the next two days ($2.5 \times 10^{-8}\ (\Omega\ \mathrm{cm})^{-1}$) which corresponds to the progressive polymer destruction as discussed in our preceding paper on bromine doping of PVK powder [16].

As conclusion it can be said that the optimum doping conditions of PVK thin films with bromine has been shown to be room temperature post-doping. However, even at room temperature there is Br–PVK covalent bonds formation, which are due to the high reactivity of bromine.

## References

[1] Hoegl H. J Phys Chem 1965;G9:255.
[2] Pearson JM, Stolka M. Poly(*N*-vinylcarbazole), Polymer monograph, vol. 6. New York: Gordon and Breach, 1981.
[3] Nguyen TP, Molinie P, Destwel P. Organic and polymer-based light-emitting diodes. In: Nahud HS, editor. Handbook of advanced electronic and photonic materials and devices, Light-emitting diodes, lithium batteries and polymer devices, vol. 10. San Diego: Academic Press, 2000.
[4] Morila D, Kitagawa M, Kusano H, Kawakami S, Isushima T, Sawada T, Hatano K, Hirooka K, Kbayashi H. Synth Met 2000;111–112:217.
[5] Gautier E, Thianche E, Sentein C, Lorin A, Denis C, Raimond P, Nunzi JM. J Appl Phys 1998;83:4236.
[6] Kido J, Shionaya H, Nagai K. Appl Phys Lett 1995;67:2281.
[7] Gyauher-Thianche E, Sentein C, Nunzi JM, Lorin A, Denis C, Raimond P. Synth Met 1997;91:323.
[8] Kusano H, Shiraishi N, Hasaka S, Kuwma I, Kitagawa M, Ichino K, Kobayashi H. Synth Met 1997;91:341.
[9] Brabec CJ, Sariuftai NS. Mater Today 2000;3:5.
[10] Gazotti WA, Noagueira AF, Girotto EM, Micasoni L, Martini M, DasNeves S, De Paoli MA. Optical devices based on conductives polymers. In: Nahud HS, editor. Handbook of advanced electronic and photonic materials and devices, Light-emitting diodes, lithium batteries and polymer devices, vol. 10. San Diego: Academic Press, 2000. p. 66.
[11] Brabec CJ, Padinger F, Hummelen JC, Janssen RAJ, Sariuftai NS. Synth Met 1999;102:861.
[12] Bernede JC, Alimi K, Safoula G. Polym Degrad Stab 1999;46:269.
[13] Alimi K, Safoula G, Bernede JC, Rabiller C. J Polym Sci, Part B: Polym Phys 1992;356:585.
[14] Safoula G, Bernede JC, Alimi K, Molinié P, Touihri S. J Appl Polym Sci 1996;60:1733.
[15] Safoula G, Touihri S, Postic M, Bernede JC, Molinié P. J Chem Phys 1997;94:1602.
[16] Safoula G, Touihri S, Bernede JC, Jamali M, Rabiller C, Molinié P, Napo K. Polymer 1999;40:531.
[17] Touihri S, Molinié P, Ouro Djobo S, Napo K, Safoula G, Bernede JC. Polym Degrad Stab 2000;69:333.
[18] Napo K, Chand S, Bernede JC, Safoula G. J Mater Sci 1992;27:6219.
[19] Touihri S, Safoula G, Bernede JC, Long R, Alimi K. Thin Solid Films 1997;304:16.
[20] Touihri S, Safoula G, Bernede JC. Polym Degrad Stab 1998;60:481.
[21] Bernede JC, Touihri S, Alimi K, Safoula G, Logoff D. Eur Polym J 1998;34:269.
[22] Napo K, Safoula G, Bernede JC, D'almeida K, Touihri S, Alimi K, Barreau A. Polym Degrad Stab 1999;66:257.
[23] D'Almeida K, Bernède JC, Marsillac S, Godoy A, Diaz FR. Synth Met 2001;122:127.
[24] Urso F. La resonance paramagnétique électronique. Paris: Dunod, 1968. p. 142.
[25] Nguyen TP, Giffard M, Molinié P. J Chem Phys 1994;100:8340.
[26] Angot A. Complements de mathématiques. Masson: Paris, 1972. p. 27.
[27] Shirley DA. Phys Rev B 1972;5:4709.
[28] Beanson G, Briggs D. High resolution XPS of organic polymers—the scienta ESCA 300 Data Base. Chichester: Wiley, 1993.
[29] Wertz JE, Balton JR. Electron spin resonance. New York: Mc Graw-Hill, 1986.